

Thermoacoustic instabilities in non zero Mach number mean flow configurations.

K. Wieczorek^{1,2*}, F. Nicoud²

¹ CERFACS - 42, Av. G. Coriolis, 31057 Toulouse Cedex 01, France

² Université Montpellier II - I3M CNRS UMR 5149,
Place Eugène Bataillon, 34095 Montpellier Cedex 05, France

Abstract

In the calculation of thermoacoustic instabilities, a common assumption is that the mean flow velocity is small enough to be considered zero. This allows to considerably simplify the equations used to describe the phenomenon of acoustic propagation. However, this zero Mach number assumption may lead to significant differences in the evaluation of the thermoacoustic modes present in the domain, especially for cases with non isentropic mean flow.

This paper presents a numerical study of the effects of the mean flow on thermoacoustic instabilities. Using the Linearized Euler Equations, a modal analysis is carried out for an academic test configuration. In order to assess the effect of the mean flow terms on the mode stability, an analysis of the disturbance energy budget is performed.

Introduction

At present, several methods are used to describe combustion instabilities. They range from powerful yet very computation-time demanding Large Eddy Simulations [1] to timesaving low-order network models [2]. An intermediate method consists in solving a set of linearized equations using a finite volume technique.

Based on the Linearized Euler Equations (LEE) as the framework to represent acoustic propagation and resonance, the assumption of a zero Mach number mean flow is often made in order to allow the formulation of a wave equation. However, when the mean flow is considered to be at rest, some physical phenomena occurring in combustion applications are not correctly represented: entropy waves (hot spots) generated in the flame region are not convected downstream and their influence outside the flame zone is therefore not taken into account. Yet, entropy modes and acoustic modes can interact in zones of accelerated mean flow, as for example in the high pressure distributor downstream of the combustion chamber. There, entropy spots can partly be converted into acoustic waves, which may then propagate upstream [3].

Specific Objectives

The configuration to be analysed in this paper consists in a tube with constant cross section containing a 1D-flame. In this configuration, entropy fluctuations are created in the flame region and then convected downstream towards the chamber outlet. In the flame region, which covers about 15 % of the domain length, these entropy perturbations can interact with the acoustic field.

The resonant eigenmodes of this configuration are calculated using the Linearized Euler Equations in a frequency domain formulation. In order to evaluate the influence of the mean flow velocity, an analysis of the disturbance energy budget as proposed by Myers [4] has been carried out.

Mathematical Formulation

Linearized Euler Equations The equations used to describe the acoustic field are derived from the conservation laws for mass, momentum and energy in the formulation:

$$\frac{D\rho}{Dt} = -\rho\nabla \cdot \mathbf{u} \quad (1)$$

$$\rho \frac{D\mathbf{u}}{Dt} = -\nabla p \quad (2)$$

$$\frac{Ds}{Dt} = \frac{rq}{p} \quad (3)$$

where ρ denotes the mean density, p the static pressure, \mathbf{u} the velocity vector and s the entropy per mass unit. The quantity $r = C_p - C_v$ is the specific gas constant of the mixture and q the rate of heat release per unit of volume. In these equations, viscous terms are neglected and the heat capacities C_p and C_v are considered constant throughout the domain.

The acoustic equations can then be derived by decomposing the instantaneous values of pressure, density, velocity vector and entropy into a steady mean flow and fluctuations of small amplitude, i.e. each of these quantities can be written as $\phi(\mathbf{x}, t) = \phi_0(\mathbf{x}) + \phi_1(\mathbf{x}, t)$, where indices 0 and 1 denote mean flow quantities and small amplitude fluctuations respectively. Introducing this decomposition into the Eqs. (1) - (3) and keeping only terms of first order leads to the Linearized Euler Equations. The fluctuating quantities are assumed to be harmonic in time, characterised by the complex frequency $\omega = \omega_r + j\omega_i$. The fluctuating quantities can then be expressed as $\phi_1(\mathbf{x}, t) = \hat{\phi}(\mathbf{x})e^{-j\omega t}$, which allows to pass to a frequency domain formulation. The configuration presented in this paper can be described with a 1D formulation of the Linearized Euler Equations, which reads:

*Corresponding author: wieczorek@cerfacs.fr
Proceedings of the European Combustion Meeting 2009

$$\begin{aligned} & \left(\frac{\partial u_0}{\partial x} + u_0 \frac{\partial}{\partial x} \right) \hat{\rho} \\ & + \left(\frac{\partial \rho_0}{\partial x} + \rho_0 \frac{\partial}{\partial x} \right) \hat{u} = j\omega \hat{\rho} \end{aligned} \quad (4)$$

$$\begin{aligned} & \left(\frac{1}{\rho_0} \frac{\partial c_0^2}{\partial x} + \frac{u_0}{\rho_0} \frac{\partial u_0}{\partial x} + \frac{c_0^2}{\rho_0} \frac{\partial}{\partial x} \right) \hat{\rho} \\ & + \left(\frac{\partial u_0}{\partial x} + u_0 \frac{\partial}{\partial x} \right) \hat{u} \\ & + (\gamma - 1) T_0 \left(\frac{1}{p_0} \frac{\partial p_0}{\partial x} + \frac{\partial}{\partial x} \right) \hat{s} = j\omega \hat{u} \end{aligned} \quad (5)$$

$$\begin{aligned} & \frac{\gamma r q_0}{\rho_0 p_0} \hat{\rho} + \frac{\partial s_0}{\partial x} \hat{u} \\ & + \left(u_0 \frac{\partial}{\partial x} + (\gamma - 1) \frac{q_0}{p_0} \right) \hat{s} - \frac{r}{p_0} \hat{q} = j\omega \hat{s} \end{aligned} \quad (6)$$

In the above equations, c_0 denotes the mean speed of sound, T_0 the mean static temperature and $\gamma = C_p/C_v$ the heat capacity ratio.

The linearized state equation and entropy expression read:

$$\frac{\hat{p}}{p_0} - \frac{\hat{\rho}}{\rho_0} - \frac{\hat{T}}{T_0} = 0 \quad (7)$$

$$\frac{\hat{s}}{C_v} = \frac{\hat{p}}{p_0} - \gamma \frac{\hat{\rho}}{\rho_0} \quad (8)$$

The unsteady heat release \hat{q} is modelled as a linear operator of the fluctuating quantities $\hat{\rho}$, \hat{u} and \hat{s} . This allows to write Eqs. (4) - (6) as an eigenvalue problem of the form

$$\mathcal{A} \vec{\mathcal{V}} = j\omega \vec{\mathcal{V}} \quad (9)$$

where the matrix \mathcal{A} is the linear operator applied to the eigenvector $\mathcal{V} = (\hat{\rho}, \hat{u}, \hat{s})^T$, and $\omega = \omega_r + j\omega_i$ the complex eigenvalue.

Flame Model The interaction between the flame and the acoustic field is described using a local $n - \tau$ -model ([5], [6], [7]). This model relates the local unsteady heat release $\hat{q}(x)$ to an interaction index $n_u(x)$, a time lag τ and a reference acoustic velocity immediately upstream of the flame $\hat{u}_{x_{ref}}$:

$$\hat{q}(x) = n_u(x) \frac{\hat{u}_{x_{ref}}}{U_{bulk}} q_{total} e^{i\omega\tau} \quad (10)$$

In this expression, the quantities U_{bulk} and q_{total} are the bulk velocity and total heat release, respectively. The local interaction index is further defined as

$$\begin{aligned} n_u(x) &= \frac{n}{\delta_f} \frac{U_{bulk}}{q_{total}} \frac{\gamma}{\gamma - 1} p_0 \\ &\text{for } x_f - \frac{\delta}{2} < x < x_f + \frac{\delta}{2}; \\ n_u(x) &= 0 \quad \text{otherwise,} \end{aligned} \quad (11)$$

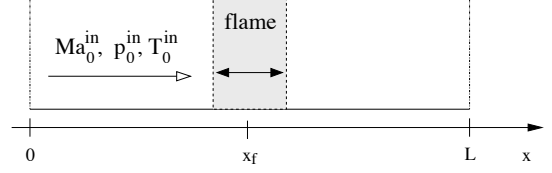


Figure 1: Test case configuration

with δ_f being the flame thickness.

Mean Flow Field The configuration presented in this paper consists in a tube of length L with constant cross section, which contains a 1D-flame of thickness δ_f at position x_f (see Fig. 1).

To account for the presence of the flame, the mean flow field is described by an analytical distribution of static temperature of the form:

$$\begin{aligned} T_0(x) &= \frac{T_0^{out} + T_0^{in}}{2} \\ &+ \frac{T_0^{out} - T_0^{in}}{2} \tanh\left(3 \frac{x - x_f}{\delta_f}\right) \end{aligned} \quad (12)$$

The conservation laws for mass flux, momentum and total temperature provide the conditions $\rho_0 u_0 = \text{const.}$, $p_0 + \rho_0 u_0^2 = \text{const.}$ and $q_0 = \rho_0 u_0 C_p dT_0/dx$.

The flow field is then entirely defined by the choice of inlet pressure p_0^{in} , temperature T_0^{in} , Mach number Ma_0^{in} and a temperature step $T_0^{out} - T_0^{in}$.

Boundary Conditions In order to solve the eigenvalue problem of Eq. (9), information about the waves entering the domain is necessary. In the presented configuration, this concerns the downstream travelling acoustic wave and the entropy wave at the domain inlet, and the upstream travelling acoustic at the domain outlet.

The boundary conditions are set as follows:

at $x = 0$:

$$\hat{s} = 0 \quad \text{and} \quad \hat{u} + u_0/(\rho_0 c_0^2) \hat{p} = 0 \quad (13)$$

at $x = L$:

$$\hat{p} + \rho_0 u_0 \hat{u} = 0 \quad (14)$$

The conditions for the acoustic waves are set in a way that the acoustic energy flux across the domain boundaries $F = (\hat{u} + u_0/(\rho_0 c_0^2) \hat{p})(\hat{p} + \rho_0 u_0 \hat{u})$ ([8]) is zero at both inlet and outlet. As for the entropy wave, the boundary condition implies that any entropy fluctuations present in the domain are created in the flame and then convected downstream.

Numeric Implementation The eigenvalue problem of Eq. (9) can be written in discrete form as

$$[A_{1D}][V_{1D}] = j\omega[V_{1D}] \quad (15)$$

where the discrete eigenvector $[V_{1D}]$ contains the unknown values of $(\hat{\rho}, \hat{u}, \hat{s})$ for each grid point. Note that in cases with unsteady heat release, the operator matrix $[A_{1D}]$ may depend on ω (via Eq. (10)). The discretised eigenvalue

problem has then to be solved iteratively.

For the generation of matrix $[A_{1D}]$, a central finite difference scheme is used to approximate gradients of $\hat{\rho}$ and \hat{u} , while gradients of \hat{s} are expressed using an upwind difference scheme. In order to avoid numerical instability, a staggered grid formulation is used, where values of \hat{u} are stored at the nodes, while $\hat{\rho}$ and \hat{s} are stored at the cell centers. A more detailed description of the mathematical and numerical formulation can be found in [9].

Disturbance Energy Budget For the eigenmodes that are solutions of the discrete problem of Eq. (15), an analysis of the disturbance energy budget is carried out in order to evaluate the influence of the non-zero Mach number mean flow on the stability of the modes.

In the presented case, both acoustic and entropy modes exist in the domain and can interact in the flame zone. To describe this configuration, the corollary for disturbance energy derived by Myers ([4]) and extended by Karimi et al. ([10]) is used. For a 1D inviscid flow, this corollary reads:

$$\frac{\partial E_2}{\partial t} + \frac{\partial W_2}{\partial x} = D_2 \quad (16)$$

with E_2 the first-order disturbance energy density, W_2 the first-order disturbance energy flux vector and D_2 the rate per unit volume of dissipation of first-order disturbance energy defined as:

$$E_2 = \frac{p_1^2}{2\rho_0 c_0^2} + \frac{\rho_0 u_1^2}{2} + \rho_1 u_0 u_1 + \frac{\rho_0 T_0 s_1^2}{2c_{p_0}} \quad (17)$$

$$W_2 = \frac{u_0}{\rho_0} p_1 \rho_1 + p_1 u_1 + u_0^2 \rho_1 u_1 + u_0 \rho_0 u_1^2 + \rho_0 u_0 T_1 s_1 \quad (18)$$

$$D_2 = -s_1(\rho_1 u_0 + \rho_0 u_1) \frac{dT_0}{dx} + s_1 \rho_0 u_0 \frac{dT_1}{dx} + T_1 \left(\frac{q_1}{T_0} - \frac{q_0 T_1}{T_0^2} \right) \quad (19)$$

This expression is then integrated in time over one period of oscillation and integrated in space over the whole domain, which yields:

$$\int E_2 dx|_{t=T} - \int E_2 dx|_{t=0} + \int W_2 dt|_{x=L} - \int W_2 dt|_{x=0} - \int \int D_2 dx dt = 0 \quad (20)$$

In the following a notation will be used, where $\langle \rangle$ denotes the time integration from $t = 0$ to $t = T$ and $\bar{\cdot}$ stands for the space integration from $x = 0$ to $x = L$. Setting the energy density initially contained in the domain as a reference value to $\overline{E_2^{t=0}} = 1$, one obtains the scaled balance:

$$\overline{E_2^{t=T}} + \langle [W_2] \rangle_{x=0}^{x=L} - \overline{D_2} = 1 \quad (21)$$

p_0^{in} (Pa)	T_0^{in} (K)	T_0^{out} (K)	γ	r (J/kgK)
101325	300	1200	1.4	287
L (m)	x_f/L	δ_f/L		
1	0.5	0.15		

Table 1: Physical parameters used for the calculations

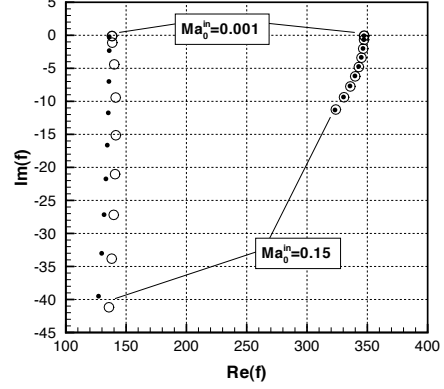


Figure 2: Passive Flame: Frequencies of 1st and 2nd mode; ●: semi-analytical method ($\delta_f \rightarrow 0$), ○: LEE ($\delta_f/L = 0.15$) for $Ma_0^{in} = 0.001$ and $Ma_0^{in} = 0.01$ to 0.15 with $\Delta Ma = 0.02$

This integrated balance is directly related to the notion of stability of the modes, in the sense that an unstable mode is characterised by increasing energy density $\overline{E_2^{t=T}} - 1 > 0$, more precisely, $E_2^{t=T} = \exp(2\omega_i T)$ holds.

Results and Discussion

The results presented in this section correspond to the configuration shown in Fig. 1 and the parameters of Table 1. The domain is discretised using between 3000 and 4000 equidistant grid points.

Passive Flame In a first time, it is supposed that no unsteady heat release occurs, i.e. $\hat{q} = 0$. The results of the calculations carried out with the LEE solver are validated using a semi-analytical model, which solves the problem for the limit case $\delta_f \rightarrow 0$ (see detailed description in [11]).

Figure 2 shows the complex eigenfrequencies of the first two modes for $Ma_0^{in} = 0.001$ and $Ma_0^{in} = 0.01$ to $Ma_0^{in} = 0.15$ with $\Delta Ma = 0.02$ obtained from the LEE solver (○-symbols) and the semi-analytical model (●-symbols). In the limit of zero mean flow Mach number, the eigenfrequencies of this configuration with the parameters $x_f/L = 0.5$ and $T_0^{out}/T_0^{in} = 4$ can be determined analytically ([12]) yielding the values $f_1 = 136.04$ Hz and $f_2 = 347.19$ Hz for the first and second mode respectively. As Fig. 2 shows, these values are obtained by both the LEE solver and the semi-analytical method. When the mean flow velocity is taken into account, both methods

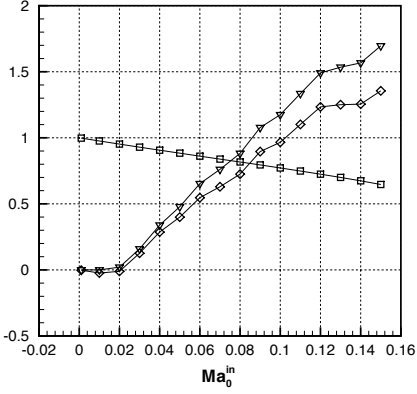


Figure 3: Passive Flame: Terms of the time and space integrated disturbance energy balance Eq. (21) for $Ma_0^{\text{in}} = 0.001$ and $Ma_0^{\text{in}} = 0.01$ to 0.15

\square : $\overline{E_2^{t=T}}$, ∇ : $\langle W_2 \rangle_{x=0}^{x=L}$, \diamond : $\langle D_2 \rangle$

predict a transition from a marginally stable ($\omega_i = 0$) to a stable mode ($\omega_i < 0$). Between $Ma_0^{\text{in}} = 0$ and $Ma_0^{\text{in}} = 0.15$, the shift in imaginary frequency obtained by the LEE solver is of -41.2 Hz for the first mode and -11.2 Hz for the second mode. The real frequency of the first mode is approximately constant, while it slightly decreases with growing inlet Mach number for the second mode. While the mean flow effect on the imaginary frequency of the first mode is slightly underestimated by the infinite thin flame approximation, the results obtained by the two methods are virtually the same for the second mode. This latter observation results from the structure of the second mode, which contains a velocity node at the position of the flame.

For the second mode of this passive flame configuration, a energy budget analysis as in Eqs. (16) - (21) has been carried out, for inlet Mach numbers of $Ma_0^{\text{in}} = 0.001$ and $Ma_0^{\text{in}} = 0.01$ to $Ma_0^{\text{in}} = 0.15$ varying in steps of $\Delta Ma = 0.01$. The results for the terms of Eq. (21) are shown in Fig. 3. In agreement with the evolution of the imaginary frequency shown in Fig. 2, the energy density contained in the domain is conserved for the case $Ma_0^{\text{in}} = 0.001$ (i.e. $\overline{E_2^{t=T}} = \overline{E_2^{t=0}} = 1$), whereas the energy density decreases during each period of oscillation as soon as $Ma_0^{\text{in}} \geq 0.01$

With the boundary conditions of Eqs. (13), (14), the flux term reduces to the contribution of the entropy fluctuation at the domain outlet, i.e.

$$\langle W_2 \rangle_{x=0}^{x=L} = \int_{t=0}^{t=T} (\rho_0 u_0 T_1 s_1)_{x=L} dt.$$

Being a function of the mean flow velocity, this term is zero for $Ma_0^{\text{in}} = 0$ and starts to play a role only when $Ma_0^{\text{in}} \geq 0.02$.

The evolution of the source term with growing Mach number follows that of the flux term. In the definition of the individual terms of $\langle D_2 \rangle$ (i.e. integrated and scaled terms of Eq. (19)), the last two terms are related to the unsteady and steady heat release of the flame respectively.

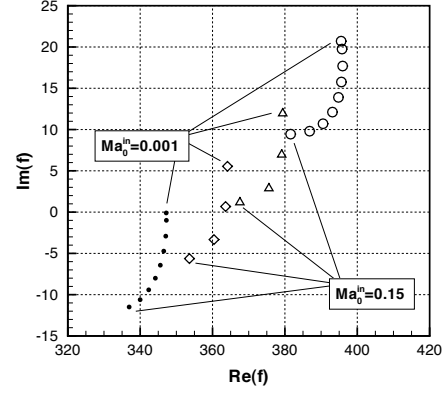


Figure 4: Active Flame, Complex frequencies of 2nd mode; \bullet : semi-analytical method ($\delta_f \rightarrow 0$), \circ : LEE ($\delta_f/L = 0.15$) for $Ma_0^{\text{in}} = 0.001$ and $Ma_0^{\text{in}} = 0.01$ to 0.15 with $\Delta Ma = 0.02$; \diamond : LEE ($\delta_f/L = 0.05$), \triangle : LEE ($\delta_f/L = 0.10$) for $Ma_0^{\text{in}} = 0.001 / 0.05 / 0.10 / 0.15$

	δ_f/L	f (Hz)
$Ma_0^{\text{in}} = 0.001$	0	347.20 - 0.10i
	5%	364.13 + 5.54i
	10%	379.40 + 11.95i
	15%	395.55 + 20.69i
$Ma_0^{\text{in}} = 0.1$	0	343.34 - 8.73i
	5%	360.40 - 3.33i
	10%	375.58 + 2.88i
	15%	391.99 + 11.35i

Table 2: Active Flame: Shift of complex eigenfrequencies for increasing flame thickness

While the unsteady heat release term is set to zero in the present passive flame case, the steady heat release term $\langle D_{2,5} \rangle = \int_{t=0}^{t=T} \int_{x=0}^{x=L} (-q_0 T_1^2/T_0^2) dx dt$ grows with increasing Mach numbers, as q_0 is proportional to the mean flow velocity. Containing a quadratic temperature fluctuation term, the integrated mean heat release term is negative as soon as $Ma_0^{\text{in}} > 0$, which means that it acts as a sink term. The overall behaviour of $\langle D_2 \rangle$ as feeding energy to the system as shown in Fig. 3 is therefore due to the contribution of its first three terms.

Active Flame In a second time, the same configuration was simulated including an unsteady heat release term as defined in Eqs. (10) and (11). The parameters of the $n - \tau$ -model are set to the values $n = 5$ and $\tau = 0.5$ ms.

The complex eigenfrequencies of the second mode for $Ma_0^{\text{in}} = 0.001$ and $Ma_0^{\text{in}} = 0.01$ to $Ma_0^{\text{in}} = 0.15$ in steps of $\Delta Ma = 0.02$ are shown in Fig. 4. In addition to the results for $\delta_f \rightarrow 0$ obtained from the semi-analytical model (\bullet -symbols) and the LEE results for a flame thickness of $\delta_f = 0.15L$ (\circ -symbols), LEE results for the

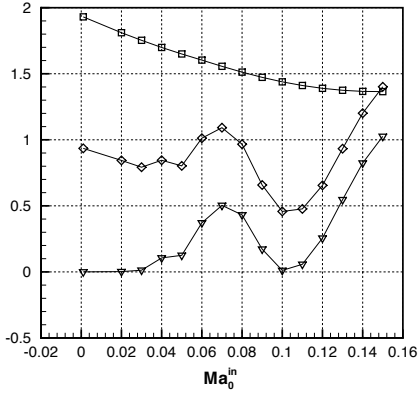


Figure 5: Active Flame: Terms of the time and space integrated disturbance energy balance Eq. (21) for $Ma_0^{\text{in}} = 0.001$ and $Ma_0^{\text{in}} = 0.01$ to 0.15 , $\delta_f/L = 0.15$
 \square : $\overline{E_2^{t=T}}$, ∇ : $[\langle W_2 \rangle]_{x=0}^{x=L}$, \diamond : $\langle D_2 \rangle$

two intermediate values of $\delta_f = 0.05L$ (\diamond -symbols) and $\delta_f = 0.10L$ (\triangle -symbols) are plotted. For the two Mach numbers of $Ma_0^{\text{in}} = 0.001$ and $Ma_0^{\text{in}} = 0.1$, the eigenfrequencies for the different values of δ_f are assembled in Table 2.

The results suggest that for a given mean flow velocity, an increase of the flame thickness leads to a higher frequency of oscillation and more instability. When the mean flow Mach number is increased, the results for the different values of δ_f agree in predicting a trend towards lower real frequencies and more stability.

For $\delta_f/L = 0.15$, an analysis of the disturbance energy budget has been carried out for the inlet Mach numbers $Ma_0^{\text{in}} = 0.001$ and $Ma_0^{\text{in}} = 0.1$ to $Ma_0^{\text{in}} = 0.15$ in steps of $\Delta Ma_0^{\text{in}} = 0.1$ (see Fig. 5). For this configuration, for all values of Ma_0^{in} the amount of energy added to the system by the source term is higher than the losses at the boundaries described by the flux term, which is in agreement with the positive values of ω_i displayed in Fig. 4.

Again, flux and source terms evolve in a similar way, with the flux term being non-zero only after $Ma_0^{\text{in}} \geq 0.03$. However, the flux term does not grow in a monotone way with the inlet Mach number, but drops down to zero at approximately $Ma_0^{\text{in}} = 0.1$. This can be explained the fact that the flux term is composed of a product of a temperature fluctuation T_1 and an entropy fluctuation s_1 , which are both assumed time harmonic. For a phase shift of $\Delta\phi = \pi/2$ between the two signals, the time integral of the product is zero.

The source term now contains a contribution of the unsteady heat release \hat{q} . This means that all the separate terms of the source term defined in Eq. (19) are involved, and it can be of interest to evaluate the different terms to get information about their order of magnitude.

Therefore, the contributions of the individual terms of the

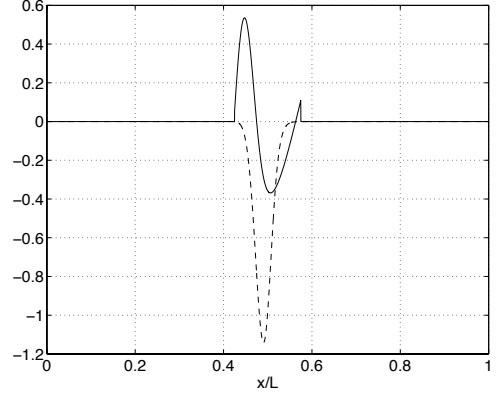


Figure 6: Local distribution of time integrated source terms $\langle D_{2,4}(x) \rangle$ (solid line) and $\langle D_{2,5}(x) \rangle$ (dashed line) for $Ma=0.1$, $\delta_f/L = 15\%$

energy balance of Eq. (21) are assembled in Table 3 for $Ma_0^{\text{in}} = 0.001$ and $Ma_0^{\text{in}} = 0.1$. The values for the case of a flame thickness of $\delta_f/L = 0.15$ discussed above are compared to those for $\delta_f/L = 0.05$ and $\delta_f/L = 0.10$. The corresponding eigenfrequencies are those of Table 2.

The results in Table 3 indicate that the integrated balance of Eq. (21) is satisfied for the presented cases. The shift towards more stable imaginary frequencies when passing from $Ma_0^{\text{in}} = 0.001$ to $Ma_0^{\text{in}} = 0.1$ observed for the three values of δ_f (see Fig. 4) is confirmed by the results for $\overline{E_2^{t=T}}$: The amount of energy density contained in the domain after one period of oscillation for $Ma_0^{\text{in}} = 0.1$ is lower than the respective value at $Ma_0^{\text{in}} = 0.001$. This trend towards more stability with higher Mach numbers is expressed by a growth of the flux term that exceeds that of the source term for $\delta_f/L = 0.05$ and $\delta_f/L = 0.10$, and a reduction of the source term with approximately constant flux term for $\delta_f/L = 0.15$.

When the mean flow Mach number is very low, only the terms $\langle D_{2,2} \rangle$ and $\langle D_{2,4} \rangle$ contribute to the disturbance energy balance, as the other terms are directly related to the mean flow velocity. Table 3 indicates that for the presented values of δ_f the source term is dominated by the unsteady heat release term $\langle D_{2,4} \rangle$.

For $Ma_0^{\text{in}} = 0.1$, all terms contribute in a non-negligible way to the energy balance. However, a clear tendency of the behaviour of these integrated terms as a function of mean flow Mach number or flame thickness can not be deduced. Except of the term related to the mean heat release, which by its definition acts as a sink term, the local contribution of all other terms can be either input or extraction of energy (see Fig. 6). After spatial integration, the overall contribution may be that of a source or a sink term.

Conclusions

A modal analysis of an academic configuration was carried out using the Linearized Euler Equations, taking into account the mean flow and a 1D flame. Compari-

δ_f/L	$Ma_0^{\text{in}} = 0.001$			$Ma_0^{\text{in}} = 0.1$		
	5%	10%	15%	5%	10%	15%
$\overline{E_2^{t=T}}$	1.21	1.49	1.93	0.89	1.10	1.44
$[\langle W_2 \rangle]_{x=0}^{x=L}$	0.00	0.00	0.00	1.14	0.75	0.01
$\overline{\langle D_2 \rangle}$	0.22	0.49	0.94	1.05	0.87	0.46
$\overline{\langle D_{2,1} \rangle} = \int \int (-s_1 \rho_1 u_0 dT_0/dx) dx dt$	0.00	0.00	0.00	0.26	0.29	0.86
$\overline{\langle D_{2,2} \rangle} = \int \int (-s_1 \rho_0 u_1 dT_0/dx) dx dt$	0.04	0.07	0.10	0.12	0.58	0.86
$\overline{\langle D_{2,3} \rangle} = \int \int (s_1 \rho_0 u_0 dT_1/dx) dx dt$	0.01	0.01	0.01	0.87	1.04	1.01
$\overline{\langle D_{2,4} \rangle} = \int \int (T_1 q_1/T_0) dx dt$	0.19	0.44	0.85	0.50	0.41	-0.13
$\overline{\langle D_{2,5} \rangle} = \int \int (-q_0 T_1^2/T_0^2) dx dt$	-0.02	-0.02	-0.02	-0.69	-1.44	-2.15

Table 3: Active Flame: Terms of time and space integrated disturbance energy balance Eq. (21), separate contributions of source term: cf. Eq (19)

son of the complex eigenfrequencies obtained by the LEE calculations to those of a semi-analytical method showed good overall agreement.

The frequency shift with increasing mean flow Mach number was predicted in the same way by the two methods: For the presented configuration, an increasing mean flow Mach number leads to more stable modes for both the passive and active flame configuration.

Active flame calculations have been carried out for different values of the flame thickness using the LEE solver. For the presented configuration, the LEE calculations predict a trend towards higher resonant frequencies and more unstable modes with increasing flame thickness.

An analysis of the disturbance energy budget confirmed the results of the LEE solver. An evaluation of the separate terms showed that source terms related to the mean flow velocity can contribute considerably to the disturbance energy balance.

Acknowledgements

The authors gratefully acknowledge the financial support provided by the European Union in the framework of the project AETHER (Contract No. FP6 - MRTN-CT-2006-035713). This work was also performed in the framework of the BRUCO project funded by the Fondation Nationale de Recherche pour l'Aéronautique et l'Espace.

References

- [1] C. Martin, L. Benoit, Y. Sommerer, F. Nicoud, T. Poinsot, Les and acoustic analysis of combustion instability in a staged turbulent swirled combustor, *AIAA Journal* 44 (4) (2006) 741–750.
- [2] S. R. Stow, A. P. Dowling, Modelling of circumferential modal coupling due to helmholtz resonators, in: *ASME Paper 2003-GT-38168*, Atlanta, Georgia, USA, 2003.
- [3] F. E. Marble, S. Candel, Acoustic disturbances from gas nonuniformities convected through a nozzle, *J. Sound Vib.* 55 (1977) 225–243.
- [4] M. K. Myers, Transport of energy by disturbances in arbitrary steady flows, *J. Fluid Mech.* 226 (1991) 383–400.
- [5] L. Crocco, Aspects of combustion instability in liquid propellant rocket motors. part i., *J. American Rocket Society* 21 (1951) 163–178.
- [6] L. Crocco, Aspects of combustion instability in liquid propellant rocket motors. part ii., *J. American Rocket Society* 22 (1952) 7–16.
- [7] F. Nicoud, L. Benoit, C. Sensiau, Acoustic modes in combustors with complex impedances and multidimensional active flames, *AIAA Journal* 45 (2007) 426–441.
- [8] R. H. Cantrell, R. W. Hart, Interaction between sound and flow in acoustic cavities: Mass, momentum, and energy considerations, *J. Acous. Soc. Am.* 36 (4) (1964) 697 – 706.
- [9] F. Nicoud, K. Wiecezorek, About the zero mach number assumption in the calculation of thermoacoustic instabilities, *International Journal of Spray and Combustion Dynamics* 1 (2009) (in press).
- [10] N. Karimi, M. Brear, W. Moase, Acoustic and disturbance energy analysis of a flow with heat communication, *J. Fluid Mech.* 597 (2008) 67–89.
- [11] A. P. Dowling, The calculation of thermoacoustic oscillations, *J. Sound Vib.* 180 (4) (1995) 557–581.
- [12] A. Kaufmann, F. Nicoud, T. Poinsot, Flow forcing techniques for numerical simulation of combustion instabilities, *Combust. Flame* 131 (2002) 371–385.